Nuclear Scattering of Nucleons and Antinucleons*

HANS-PETER DUERR†
Department of Physics, University of California, Berkeley, California
(Received October 28, 1957)

Total cross sections and reaction cross sections for scattering of nucleons and antinucleons from nuclei are calculated in the WKB approximation. The real part of the potential is the effective potential of the relativistic theory proposed in earlier papers, with a radial dependence consistent with the electron scattering results. The absorption coefficient is related to the observed particle-particle cross sections in the usual fashion. The resulting cross sections for nucleons agree quite well with the experimental data up to approximately 250 Mev. However, the high-energy nucleon total cross section and the antinucleon cross sections are too large. This discrepancy presents a real difficulty for the relativistic theory.

I. INTRODUCTION

IN an earlier paper[1] a nuclear model was developed in which the binding forces were derived from very strong interactions with scalar and vector meson fields. In the nonrelativistic limit the effective potential in this model consists of a static part and a velocity-dependent part which results from the scalar field interaction. Owing to this velocity dependence, saturation of the nuclear forces can be established. The nucleons then behave in the nucleus as if they only had about one-half of their normal mass. Brueckner *et al.*[2] have arrived at this same result from a completely different point of view.

In our model the velocity-independent part of the potential is a partial cancellation of two very strong interactions. Therefore the quantities which involve the sum rather than the difference of these strong interactions are of special interest. These quantities should exhibit large effects which may be detected experimentally. The spin-orbit coupling was found to have this property, and its large strength, indeed, was demonstrated a long time ago by the success of the shell model and the nuclear polarization experiments. Similarly the interaction between antinucleons and nuclei should be stronger than the interaction of nucleons with nuclei. On this basis we predicted large antiproton-nuclei cross sections, which then were observed. However, the previous estimate of this cross section was only very rough, and, in this paper, will be recalculated with more realistic assumptions about the nuclear surface. We also shall compute the nucleon-nucleus cross sections up to very high energies. Since the scalar interaction becomes very weak at high energies, the effective potential in our model becomes strongly repulsive. This will have an important effect on the cross sections.

In part II we describe briefly the approximations employed in the calculation. In subsequent parts we elaborate somewhat on our choice of the real part of the potential and the absorption coefficient. In part V we shall give the results and discuss their dependence on the various parameters. In part VI we shall draw our conclusions.

II. WKB APPROXIMATION

For the calculation of the cross section we employ the WKB approximation which is valid if the wavelength of the incident particle is much smaller than the surface thickness of the potential, or, in more quantitative terms, if the energy of the incident particle E' is much bigger than $m[0.2\alpha\lambda\!\!\!^{-}_c v_{\rm eff}]^{\frac{2}{3}}$, where $v_{\rm eff}$ is the effective potential measured in units of the nucleon mass m, $\lambda\!\!\!^{-}_c$ is the nucleon Compton wavelength and α the slope parameter of the effective potential. Here and in the following we set $\hbar=c=1$. For a potential depth of about 50 Mev ($v_{\rm eff}\approx 0.05$) and a slope parameter $\alpha=0.4/\lambda\!\!\!^{-}_c\approx 2\times 10^{+13}$ cm^{-1} this gives $E'\gg 0.025\ m$; i.e., for energies much larger than 25 Mev the WKB approximation should be valid in this case.

The real part of the phase shift of the lth partial wave is given in the WKB approximation:

$$\delta_l^{(r)}=\int_{r_2}^{\infty} k_i\left[1-\frac{(l+\frac{1}{2})^2}{k_i^2 r^2}\right]^{\frac{1}{2}} dr - \int_{r_1}^{\infty} k\left[1-\frac{(l+\frac{1}{2})^2}{k^2 r^2}\right]^{\frac{1}{2}} dr, \quad (1)$$

with

$$r_1=(l+\tfrac{1}{2})/k, \quad r_2=(l+\tfrac{1}{2})/k_i(r_2), \quad (2)$$

where $k_i(r)$ and k are the wave numbers (or momenta) of the impinging particle inside and outside the potential respectively. For the imaginary part of the phase shift of the lth partial wave, we have

$$\delta_l^{(i)}=\tfrac{1}{2}\int_{r_2}^{\infty} dr \frac{K(r)}{[1+(l+\frac{1}{2})^2/k_i^2 r^2]^{\frac{1}{2}}}, \quad (3)$$

where $K(r)$ is the absorption coefficient as a function of the radius variable. In Eq. (3) we do not replace

* Work supported in part by Office of Ordnance Research, U. S. Army, and in part by Deutsches Bundesministerium für Atomfragen.
† Address after January 15, 1958: Max-Planck-Institut, Göttingen, Germany.
[1] H. P. Duerr, Phys. Rev. **103**, 469 (1956), hereafter referred to as I.
[2] Brueckner, Mahmoud, and Levinson, Phys. Rev. **95**, 217 (1954).

$k_i(r)$ by k which is commonly done. This replacement corresponds physically to a straight path approximation of the particle orbit. Equation (3) gives the phase shift along the actual orbit. For very high energies this correction is irrelevant. From the real and imaginary part of the phase shifts we obtain the cross sections in the usual way. The total cross section and reaction cross section are, respectively, given by

$$\sigma_t=\frac{2\pi}{k^2}\sum_{l=0}^{\infty}(2l+1)[1-\exp(-2\delta_l^{(i)})\cos 2\delta_l^{(r)}], \quad (4)$$

$$\sigma_r=\frac{\pi}{k^2}\sum_{l=0}^{\infty}(2l+1)[1-\exp(-4\delta_l^{(i)})]. \quad (5)$$

III. EFFECTIVE POTENTIAL

In our theory the effective potential for nucleons and antinucleons in the WKB approximation is given by Eqs. (92) and (95) in I, respectively, which can be combined in the form

$$v_{\text{eff}}=|\epsilon|-[(\epsilon-b\phi_0)^2+a\phi(2-a\phi)]^{\frac{1}{2}}, \quad (6)$$

where ϵ is the total energy of the particle measured in units of the nucleon mass and is taken positive for nucleons and negative for antinucleons; a and b are constants which are related to the coupling constants of the scalar and vector fields $\phi(r)$ and $\phi_0(r)$, respectively.

$\phi(r)$ and $\phi_0(r)$ are derived from the nuclear density distribution, and in the case of zero range are given by (35) and (36) in I, i.e.,

$$\phi=\left(1-\frac{1}{\gamma^2}\frac{E_k^0}{m}\right)\frac{am}{\mu_1^2}\rho, \quad (7)$$

$$\phi=\frac{bm}{\mu_2^2}\rho. \quad (8)$$

Here E_k^0 is the average kinetic energy of the nucleons of normal mass in the nucleus, $\gamma=1-a\phi$ is the mass reduction factor, and μ_1 and μ_2 the masses of the scalar and vector mesons, respectively. For the nuclear density $\rho(r)$, we assume a Fermi distribution

$$v_\rho(r)=\{1+\exp[\alpha_\rho(r-R_\rho)]\}^{-1}, \quad (9)$$

with $r_\rho=R_\rho A^{-\frac{1}{3}}=1.07\times10^{-13}$ cm and $\alpha_\rho=1.83\times10^{+13}$ cm^{-1}, as suggested by the electron scattering experiments.[3] In particular we set

$$\rho(r)=\frac{3A}{4\pi R_\rho^3}\frac{v_\rho(r)}{[1+\pi^2/\alpha_\rho^2R_\rho^2]}, \quad (10)$$

which insures that

$$\int\rho(r)d\tau=A.$$

ϕ and ϕ_0 are essentially proportional to the ρ distribution and we therefore simply assume a similar radial dependence for these functions, i.e.,

$$\phi(r)=\phi^0v_\phi(r), \quad (11)$$

$$\phi_0(r)=\phi_0{}^0v_\phi(r), \quad (12)$$

with

$$v_\phi(r)=\{1+\exp[\alpha_\phi(r-R_\phi)]\}^{-1}. \quad (13)$$

ϕ^0 and $\phi_0{}^0$ are the strengths of the scalar and vectors fields inside the infinite nucleus as calculated in I and in another paper.[4] However, to allow for the finite range of the interaction (which for simplicity we assume to be the same for the scalar and vector fields) we use for α_ϕ and R_ϕ values different from α_ρ and R_ρ. In particular we shall consider two extreme cases:

1. The interaction between nucleons is of the form of a Yukawa potential of meson mass μ which will yield approximately

$$R_\phi=R_\rho, \quad \alpha_\phi^{-1}=\alpha_\rho^{-1}+\mu^{-1}. \quad (14)$$

2. The interaction between nucleons is constant over a range d and zero outside which gives

$$R_\phi=R_\rho+d, \quad \alpha_\phi=\alpha_\rho. \quad (15)$$

If we take for the constants a and b the values determined in II for the infinite nucleus with radius parameter $r_0=1.07\times10^{-13}$ cm,

$$a\phi^0=0.439, \quad b\phi_0{}^0=0.347, \quad (16)$$

the effective potential becomes

$$v_{\text{eff}}(r)=|\epsilon|-[\epsilon^2-(0.878-0.6934\epsilon)v_\phi(r)-0.0725v_\phi^2(r)], \quad (17)$$

with the physical restrictions on the radius and the slope parameter

$$R_\phi>R_\rho=1.07\times10^{-13}A^{\frac{1}{3}}\text{ cm}, \quad \alpha_\phi<\alpha_\rho=1.83\times10^{+13}\text{ cm}^{-1}. \quad (18)$$

For each energy Eq. (17) represents the equivalent static potential. The shapes of these potentials are given for several energies in Fig. 1 for a radius $R_\phi=6.93\times10^{-13}$ cm and $\alpha_\phi=1.83\times10^{+13}$ cm^{-1} (Pb). The effective potential is approximately a Fermi distribution function. The radius and slope parameter will in general, depend on the energy. Using the parameters of Eq. (16), we find that for small energies the halfway radius of the effective potential is

$$R_{50\%}=R_\phi+\alpha_\phi^{-1}[0.63+0.0034E'], \quad (19)$$

where E' is the energy measured in Mev. The points at which the potential assumes 90% and 10% of its central value are given, respectively, by

$$R_{90\%}=R_\phi+\alpha_\phi^{-1}[2.74+0.0029E'], \quad (20)$$

$$R_{10\%}=R_\phi+\alpha_\phi^{-1}[-1.33+0.0065E']. \quad (21)$$

[3] Hahn, Ravenhall, and Hofstadter, Phys. Rev. **101**, 1131 (1956).

[4] H. P. Duerr, Phys. Rev. **109**, 117 (1958), hereafter referred to as II.

These equations imply that the slope parameter for small energies is

$$\alpha=1.08[1+0.0009E']\alpha_\phi. \tag{22}$$

With $\alpha_\phi=1.83\times10^{+13}$ cm^{-1}, for example, one gets

$$R_{50\%}=R_\phi+[0.35+0.0019E']\times10^{-13}\text{ cm},$$
$$\alpha=1.96[1+0.001E']\times10^{+13}\text{ cm}^{-1}.$$

For energies higher than $\approx$50 Mev, however, the surface becomes more and more asymmetrical with respect to the half-way point owing to the development of a dip close to the surface. The potential is steeper between the 50% and 90% points than between the 50% and 10% points. The mean square radius of this potential is larger than the mean square radius of the corresponding Fermi function with the parameters given by Eqs. (19) and (22). For very high energies the repulsive potential has a Fermi shape and the same radius and slope parameter as the function $v_\phi(r)$. The wave numbers or momenta of the particle inside and outside the nucleus in Eqs. (1) and (3) are related to the effective potential and the energy in the usual way; i.e., in our notation,

$$k_i=m\{[|\epsilon|-v_{\text{eff}}(r)]^2-1\}^{\frac{1}{2}}, \tag{23}$$

$$k(r)=m[\epsilon^2-1]^{\frac{1}{2}}. \tag{24}$$

In the effective potentials discussed above we have not included terms which are proportional to the gradient of the potential. Although these can be neglected in the classical approximation they can easily be incorporated. If we go back to the nonrelativistic Hamiltonian [Eq. (78) in I], we can show that the effective potential is approximately given by

$$v_{\text{eff}}'=v_{\text{eff}}+\frac{\lambda\!\!\!^{-}_c{}^2}{8\gamma}\left[\nabla^2(a\phi+b\phi_0)+\frac{2}{\gamma}(\nabla a\phi)(\nabla b\phi_0)\right], \tag{25}$$

where v_{eff} is the effective potential discussed above. If we neglect second derivatives with respect to r we can write (25) in the form

$$v_{\text{eff}}'=v_{\text{eff}}+\frac{\lambda\!\!\!^{-}_c{}^2}{4\gamma^0}\left[\frac{1}{r}\frac{d}{dr}(a\phi+b\phi_0)+\frac{1}{\gamma}\left(\frac{d}{dr}a\phi\right)\left(\frac{d}{dr}b\phi_0\right)\right]. \tag{26}$$

The first term in the square bracket lowers the potential, whereas the second (smaller) term increases the potential at the surface; thus they produce a small dip at the surface of depth

$$\nabla v_{\text{eff}}{}^{\max}=-\tfrac{1}{4}\left(\frac{\lambda\!\!\!^{-}_c}{R_\phi}\right)(\alpha_\phi\lambda\!\!\!^{-}_c)\frac{a\phi^0+b\phi_0{}^0}{\gamma^0}$$
$$\times\left[1-\frac{(a\phi^0)(b\phi_0{}^0)}{4\gamma_0{}^0(a\phi^0+b\phi_0{}^0)}\alpha_\phi R_\phi\right]. \tag{27}$$

With the parameters of Eq. (16), we get

$$\nabla v_{\text{eff}}{}^{\max}=-0.35\left(\frac{\lambda\!\!\!^{-}_c}{R_\phi}\right)(\alpha_\phi\lambda\!\!\!^{-}_c)\left[1-\frac{\alpha_\phi R_\phi}{11.6}\right].$$

This is of the order of the spin-orbit energy which we neglect throughout this discussion, and adds to the asymmetry around the half-way point mentioned above. It is of some importance for bound states and possibly for low-energy scattering. For heavy elements, e.g., lead, it always will be negligible.

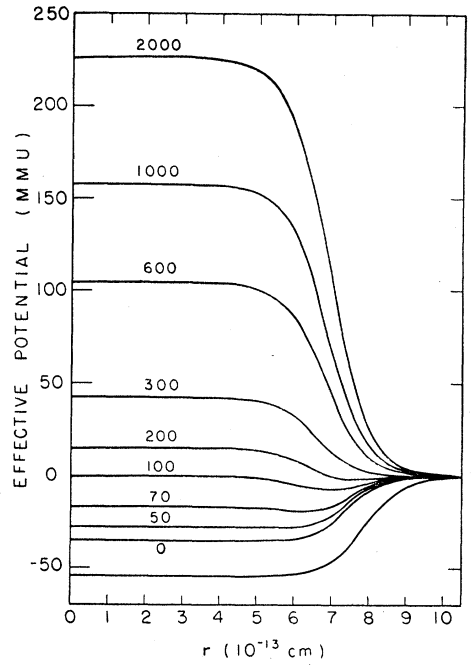

FIG. 1. The effective potential v_{eff} of a nucleus (Pb) with radius $R_\phi=6.93\times10^{-13}$ cm and slope parameter $\alpha_\phi=1.83\times10^{+13}$ cm^{-1} is plotted as a function of the radius variable r, for nucleon energies between 0 and 2000 Mev. Note that the lower curves have been mislabeled, the lowest curve having none at all. Starting from the bottom, the energies are 0, 50, 70, 100, 150, $\cdots$ Mev.

IV. ABSORPTION COEFFICIENT

The absorption coefficient K is calculated in the usual fashion from the free particle-particle total cross sections

$$K(r)=\bar{\sigma}\rho'(r). \tag{28}$$

The effective cross section $\bar{\sigma}$ is a weighted average of the proton-proton and proton-neutron total cross sections, reduced, however, by a factor which takes into account the Pauli exclusion principle. We use for this factor the expression given by Goldberger[5] (which is only valid for isotropic scattering in the center-of-mass system!)

$$f_{\text{ex}}{}^{(N)}=\left(1-\frac{7}{5}\frac{k_F{}^2}{k_i{}^2}\right)\quad(k_i>\sqrt{2}k_F), \tag{29}$$

[5] M. L. Goldberger, Phys. Rev. **74**, 1268 (1948); Hayakawa, Kawai, and Kikuchi, Progr. Theoret. Phys. (Japan) **13**, 415 (1955).

where for k_i we use the momentum of the particle at the center of the nucleus. If we assume for the calculation of the Fermi momentum k_F a "realistic" radius parameter $r_0 \approx 1.2\times10^{-13}$ cm ($E_F \approx 32$ Mev), one gets

$$f_{\mathrm{ex}}^{(N)} = 1 - \frac{0.096}{k_i^2(0)}. \tag{30}$$

For antinucleons the effect of the Pauli principle is smaller than for nucleons since that part of the total cross section which corresponds to annihilation is not reduced by the exclusion principle. For the scattering part of the cross section the reduction is less than for nucleons since only the target nucleon has to be outside the Fermi momentum sphere after collision. One easily finds, assuming again isotropic scattering, for $k_i > k_F$

$$f_{(\mathrm{ex})}^{(A)} = 1 - \frac{3}{5}\frac{k_F^2}{k_i^2(0)}. \tag{31}$$

With our choice of the Fermi momentum this leads to

$$f_{\mathrm{ex}}^{(A)} = 1 - \frac{0.041}{k_i^2(0)}. \tag{32}$$

For the effective cross section $\bar{\sigma}$ we therefore take for the various cases:

1. Neutron scattering ($\sigma_{nn} = \sigma_{pp}$):

$$\bar{\sigma} = f_{\mathrm{ex}}^{(N)}\left(\frac{Z}{A}\sigma_{np} + \frac{N}{A}\sigma_{pp}\right). \tag{33}$$

2. Proton scattering:

$$\bar{\sigma} = f_{\mathrm{ex}}^{(N)}\left(\frac{Z}{A}\sigma_{pp} + \frac{N}{A}\sigma_{np}\right). \tag{34}$$

3. Antiproton scattering:

$$\bar{\sigma} = f_{\mathrm{e}}^{(A)}(\sigma_{p\bar{p}} - \sigma_{p\bar{p}}^{\mathrm{ann}}) + \sigma_{p\bar{p}}^{\mathrm{ann}}. \tag{35}$$

For the total proton-proton and neutron-proton cross section σ_{pp} and σ_{np}, respectively, the experimental values were taken for each energy without further corrections.[6] The total proton-antiproton cross section $\sigma_{p\bar{p}}$ was taken to be 180 mb which is approximately twice the annihilation cross section $\sigma_{p\bar{p}}^{\mathrm{ann}} = 89$ mb, recently measured in proton-antiproton experiments.[7]

In Eq. (28) $\rho'(r)$ is not simply the nucleon density distribution. The effect of the finite range of nuclear forces has to be taken into account.[8] Thus we take the same functional form as $\rho(r)$ but replace R_ρ by R_ϕ and α_ρ by α_ϕ. Hence

$$K(r) = K_0 v_\phi(r), \tag{36}$$

with

$$K_0 = \bar{\sigma}\frac{3A}{4\pi R_\phi^3[1 + (\pi^2/\alpha_\phi^2 R_\phi^2)]}. \tag{37}$$

The real and imaginary part of the propagation vector therefore contain the same form factor v_ϕ of Eq. (13). In Fig. 2 the absorption coefficient in the center of the nucleus, K_0, is shown as a function of energy for neutrons in Pb, Cu, and Al and for protons in Pb.

V. RESULTS AND DISCUSSION

If we take for $a\phi^0$ and $b\phi_0{}^0$ the values in Eq. (16), which give the correct volume energy for bound states,[4] and if we assume the absorption coefficient to be derived from the particle-particle cross sections as given above, the only parameters to be determined are the radius and the slope parameters in v_ϕ. Their choice, however, is limited by the inequalities in (18). We have established these parameters by comparison with the measured reaction cross sections for lead. In one case we set $R_\phi = 1.07\times10^{-13} A^{\frac{1}{3}}$ cm and choose $\alpha_\phi = 1.3\times10^{+13}$ cm^{-1} in order to fit the Pb-reaction cross section. In the second case we choose $\alpha_\phi = 1.83\times10^{+13}$ cm^{-1} and found R_ϕ to be equal to $(1.07\,A^{\frac{1}{3}} + 0.6)\times10^{-13}$ cm. The two reaction cross-section curves in Fig. 2 are not very different. With all the parameters fixed we then calculated the reaction and total cross section for nucleons, and the reaction, annihilation and total cross section for antinucleons, from 50 to 2000 Mev. The calculations were made on the University of California IBM 701 electronic computer.[9] The results

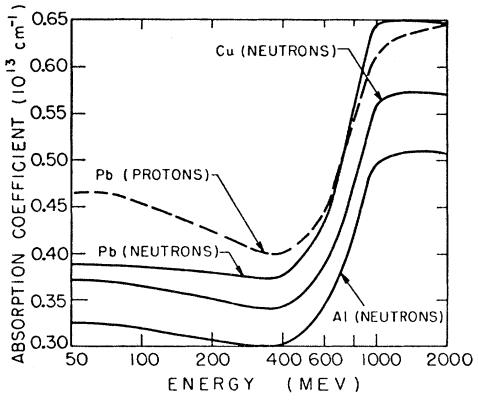

FIG. 2. The absorption coefficient in the center of the nucleus, K_0, as derived from the experimental particle-particle cross sections, is plotted *vs* the energy for neutrons in Pb, Cu, and Al, and for protons in Pb.

[6] Summary by Hildebrand, Hicks, and Harker, University of California Radiation Laboratory Report UCRL-1305, 1951 (unpublished); Chen, Leavitt, and Shapiro, Phys. Rev. **103**, 211 (1956); Chamberlain, Pettengill, Segrè, and Wiengand, Phys. Rev. **93**, 1424 (1954); **83**, 923 (1951); Kruse, Teem, and Ramsey, Phys. Rev. **94**, 1795 (1954); **101**, 1079 (1956); Coor, Hill, Hornyak, Smith, and Snow, Phys. Rev. **98**, 1369 (1955).

[7] Chamberlain, Keller, Mermod, Segrè, Steiner, and Ypsilantis, University of California Radiation Laboratory Report UCRL-3876, 1957 (unpublished).

[8] R. W. Williams, Phys. Rev. **98**, 1387 (1955).

[9] We acknowledge the financial assistance of the National Science Foundation in obtaining the necessary computing time.

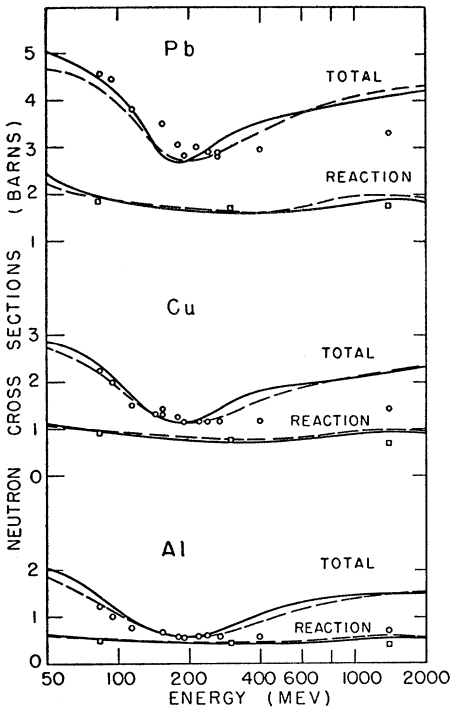

FIG. 3. The reaction cross sections and total cross sections for neutron scattering from Pb, Cu, and Al are plotted *vs* neutron energy for two cases: (1) $R_\phi=(1.07A^{\frac{1}{3}}+0.6)\times10^{-13}$ cm and $\alpha_\phi=1.83\times10^{+13}$ cm^{-1} (solid line); (2) $R_\phi=1.07A^{\frac{1}{3}}\times10^{-13}$ cm and $\alpha_\phi=1.3\times10^{+13}$ cm^{-1} (broken line). The dots indicate the experimental values.

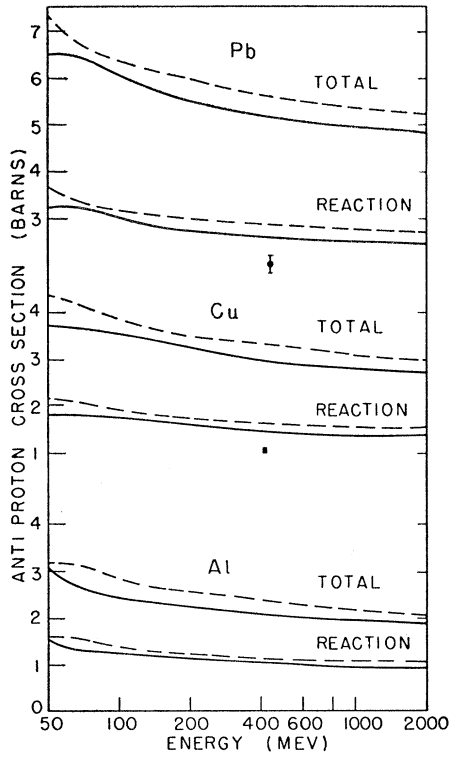

FIG. 4. The reaction cross section and total cross section for antinucleon scattering from Pb, Cu, and Al are plotted *vs* the antinucleon energy for two cases: (1) $R_\phi=(1.07A^{\frac{1}{3}}+0.6)\times10^{-13}$ cm and $\alpha_\phi=1.83\times10^{+13}$ cm^{-1} (solid line) and (2) $R_\phi=1.07A^{\frac{1}{3}}\times10^{-13}$ cm and $\alpha_\phi=1.3\times10^{+13}$ cm^{-1} (broken line). The experimental annihilation cross section for Pb and Cu are indicated by the dot and diamond, respectively.

and experimental data[10] are shown in Figs. 3 and 4 for Pb, Cu, and Al, and will now be discussed.

A. Reaction Cross Section for Nucleons

The experimental values of the reaction cross section for nucleons are more or less constant over the whole energy range considered. The calculated cross sections are somewhat larger for high energies and also in case of Pb for low energies. The deviation at high energies may be due to the neglect of some forward inelastic scattering in the experimental measurements, which are made with poor geometry. On the other hand we use Goldberger's exclusion principle factor which will underestimate the effect if the nucleon-nucleon scattering is very anisotropic in the center-of-mass system. For very high energies the scattering is actually strongly peaked forward and hence the absorption coefficient should probably be smaller.[11] The increase of the reaction cross section at low energies is mainly due to the fact that the orbits of the impinging nucleons are bent towards the nucleus. This effect will depend on the ratio of the nuclear radius to the radius of curvature of the orbit and so especially shows up in case of heavy nuclei. However, the WKB approximation may be already quite poor in that region.

We observe that a slightly larger radius parameter would be necessary (perhaps $r_\phi=R_\phi/A^{\frac{1}{3}}=1.15\times10^{-13}$ cm) to make the Al and Pb curves agree better with the experimental data for intermediate energies where the exclusion principle error is certainly smallest.

The theoretical reaction cross sections for protons deviate only slightly from the neutron values. They are about 40 to 60 mb higher than the neutron values between 50 and 400 Mev in case of Pb.

B. Total Cross Sections for Nucleons

The agreement with experimental data is quite good for small energies. Again a slightly larger radius parameter would yield better agreement. For energies higher than 250 Mev the agreement with experiment becomes gradually worse. The absolute deviation from the experimental points is roughly the same for all elements and is due to the appearance of the strong repulsive potential at high energies in our theory.

[10] Marshall, Marshall, and Nedzel, Phys. Rev. **91**, 767 (1953); J. M. Cassels, and J. D. Lawson, Proc. Phys. Soc. (London) **A67**, 125 (1954); Milburn, Birnbaum, Crandall, and Schecter, Phys. Rev. **95**, 1268 (1954); Coor, Hill, Hornyak, Smith, and Snow, Phys. Rev. **98**, 1369 (1955); V. A. Nedzel, Phys. Rev. **94**, 174 (1954); W. P. Ball, University of California Radiation Laboratory Report UCRL-1938 (unpublished).

[11] W. Heckrotte (private communication).

Owing to the strong absorption inside the nucleus only the part of the potential which is close to the surface will contribute effectively. This effect can be decreased by choosing a smaller effective radius or a steeper slope $\alpha > 1.83$ for the real part of the potential.

A small dip in the potential near the surface has the same effect upon the curves that results from an increase in well depth. In each case one finds that the low-energy part of the curves will be shifted towards higher energies.

In the case of Pb the total cross section for protons is about 130 to 150 mb larger than the neutron cross section for energies between 150 and 300 Mev, and much less for energies below and above this range.

C. Reaction and Annihilation Cross Section for Antinucleons

The reaction cross section decreases with increasing energy in a way expected from earlier investigations. The annihilation cross section is calculated in the same fashion as the reaction cross section by replacing the absorption coefficient by the annihilation coefficient $K^{\text{ann}}=\sigma_{p\bar{p}}{}^{\text{ann}}\rho'(r)$. It is smaller than the reaction cross section by about 20 mb for 100 Mev and 180 mb for 2 Bev in case of $\alpha_\phi=1.83\times10^{+13}$ cm^{-1}, and 90 mb for 100 Mev and 300 mb for 2 Bev in case of $\alpha_\phi=1.3\times10^{+13}$ cm^{-1}. The difference between the reaction and annihilation cross section is accounted for by inelastic scattering.

The calculated annihilation cross sections are larger than the experimental antiproton values, in particular by 0.66 b ($\alpha_\phi=1.3\times10^{+13}$ cm^{-1}) and 0.53 b ($\alpha_\phi=1.83\times10^{+13}$ cm^{-1}) for Pb, and 0.43 b ($\alpha_\phi=1.3\times10^{+13}$ cm^{-1}) and 0.40 b ($\alpha_\phi=1.83\times10^{+13}$ cm^{-1}) for Cu. The main reason for the large cross section is the strong annihilation in the nuclear surface region rather than the curvature of the antinucleon orbits, which was the only effect considered in our earlier estimates. The latter contribution can be decreased if one chooses a smaller radius or a steeper slope for the real part of the potential. The surface effect is illustrated by the difference in cross section in the two cases given in Fig. 4. The steeper slope leads to smaller values.

D. Total Cross Section for Antinucleons

The antinucleon total cross sections also decrease with energy in the expected way and are roughly twice the reaction cross sections.

VI. CONCLUSIONS

In comparing the theory with experiment we observe two outstanding discrepancies: (1) the calculated total cross sections for neutrons above 250 Mev are too large, and (2) the calculated annihilation cross sections for antiprotons at about 400 Mev are also too large. This disagreement indicates the absence of the strong interaction which is basic to our theory. We find that the calculations are quite sensitive to the assumptions made about the nuclear surface. Perhaps the inclusion of the space-like components of the vector field or a much more complicated relationship between nuclear density and the meson fields could reduce the strength of the effective potential at the surface.

The agreement with experiment at low energies is not relevant to the question whether our relativistic formulation of nuclear forces is valid. The absence of experimental evidence of a strong interaction in the Bev range is however a convincing prima facia argument against our relativistic formulation.

ACKNOWLEDGMENTS

I would like to thank Professor E. Teller for his continued interest and encouragement during this work, and Dr. R. D. Lawson and Dr. A. E. Glassgold for many helpful discussions and assistance in preparing the manuscript. The author also would like to acknowledge the assistance of Mr. Peter Cziffra in several numerical calculations and Mr. Ted Ross of the University of California Computing Center for valuable guidance in coding the problem.